

# The influence of temperature on Mode II fracture toughness using the Punch-Through Shear with Confining Pressure experiment

T. Meier, T. Backers & O. Stephansson  
*GeoFrames GmbH, Potsdam, Germany*

**ABSTRACT:** The influence of temperature on Mode II fracture toughness was determined using the Punch-Through Shear with Confining Pressure (PTS\CP) experiment. A total of 30 experiments was carried out and the temperature was varied from 25 to 250°C. Ultrasonic measurements before and after heating provided a basis to estimate the microcrack density development during the heating stages. It is shown that significant thermal microcracking occurs at  $T > 150^\circ\text{C}$  and that the tested fine-grained granite shows an anisotropy of approximately 15%. Experimental results show that Mode II fracture toughness remains roughly constant up to 150°C and increases slightly by 10% for elevated temperatures. The increase corresponds to the onset of thermal microcracking.

## 1 INTRODUCTION

A commonly employed way to analyse stability of constructions in geomaterials is to compare strength and stress state. If the acting stresses exceed the strength, failure is expected. This phenomenological approach bares several limitations. For example, if determining the strength parameters of rock material, one faces the problem that the values are valid strictly for the applied boundary conditions only. Hence, an increase in volume of the tested material usually results in a change, i.e. a reduction of strength. This limits the applicability of such data.

An alternative to the empirical continuum mechanics strength criteria are fracture mechanics based approaches. Linear fracture mechanics assumes pre-existing discontinuities in a material that act as stress concentrators. The magnitude of stress concentration governs the brittle fracture process. If pre-existing cracks or flaws are propagated by the stresses and coalesce to form larger discontinuities, the structures may loose integrity and fail. The mechanistic approaches try to mirror the physical origin of the processes and are therefore more exact.

Based on the principles of fracture mechanics, it is possible to not only assess the stability and safety of underground constructions, like caverns, tunnels or boreholes, but also to simulate – based on physical principles – the development of fractures in the vicinity of such openings. From the simulations the geometry of fracture patterns might be derived and used for different aspects, like fluid flow simulations or to estimate the brittle damage in underground constructions. Some software packages are already available, e.g. Fracod2D (Stephansson et al., 2008), or under development (Byfut et al., 2009).

Linear fracture mechanics provides the tools to estimate the stress and displacement fields around the tip of a fracture. Cracks or fractures are usually subdivided into three basic types, namely Mode I, Mode II and Mode III, based on the crack surface displacement (Lawn, 1993; Fig. 1 A). In Mode I, the tensile mode, the crack tip is subject to displacements perpendicular to the crack plane. In Mode II the crack faces move relatively to each other in the crack plane.

Shear traction parallels the cracking direction. In Mode III, which is relevant in three-dimensional analysis only, the shear displacement is acting parallel to the front in the crack plane. Any combination of the three basic modes is referred to as mixed mode. The principle of superposition is sufficient to describe the most general case of crack tip deformation (Whittaker et al., 1992). Loading of a fracture will always result in an alteration of the stresses at the fracture tip. In the theory of fracture mechanics, the stress intensity factor  $K_k$  (subscript  $k$  indicating the mode of loading) is a measure of the grade of stress concentration at the tip of a crack (c.f. Fig. 1 B) of effective length  $a$  at a given loading and has the dimension of stress  $\cdot$  (length)<sup>1/2</sup>, in units MPa√m, (e.g. Atkinson, 1987)

$$K_k = S_A \sqrt{\pi \cdot a} = S_{i,j} \sqrt{2\pi \cdot r} \quad (1)$$

where  $S_A$  is the applied 'far-field' stress. The stress field in front of the fracture at distance  $r$  is described by  $S_{i,j}$ . The fracture toughness  $K_{kC}$  is the limit of local stress increase due to an existing fracture at onset of critical extension.

Laboratory work in fracture mechanics is mainly based on the determination of the rocks resistance towards fracturing, which is influenced by several boundary conditions, like e.g. water content of the rock or temperature. Several studies have analysed the influence of temperature on Mode I fracture toughness (Balme et al. 2004, Dwivedi et al. 2000, Nasserri et al. 2007), but there is little to no data available on  $K_{IIIC}$  (Al-Shayea et al. 2000).

It is reported that Mode I fracture toughness is showing different behaviour for different rocks and temperature ranges. Dwivedi et al. (2000) indicated  $K_{IC}$  to increase for several rock types with decreasing temperature (+30° to -50°C). They relate this effect to the remaining moisture content in the samples. The water freezes and the fracture toughness of the ice adds to the one of the rock. Varying the moisture content changes the degree of  $K_{IC}$ -variation with temperature change. Meredith & Atkinson (1985) measured  $K_{IC}$  on plutonic rocks. For temperatures up to 100°C  $K_{IC}$  increases slightly for Westerly granite and Black gabbro (Meredith & Atkinson op. cit.) and decreases at further elevated temperatures. The increment of  $K_{IC}$  at relative low temperatures is related to the first thermally induced microcracks. These cracks are relative small in number, isolated and with no preferred orientation. They do not enhance the formation of a macrocrack; on the contrary they act as arrester to the macrocrack propagation. Therefore, a higher energy is needed to overcome this obstacle.

The closing of pre-existing cracks due to different thermal expansion of grains and an associated increasing value of fracture toughness is comprised in the term crack closure toughening. Balme et al. (2004) studied this effect on tempered Icelandic basalt containing a high amount of pre-existing cracks that seem to be closed at  $T = 150^\circ\text{C}$ . In the broadest sense, Funatsu et al. (2004) experienced crack closure toughening on clay bearing sandstone, too. During heating the amount of pore water was considerably decreased, increasing the friction in the rock and, hence, increasing  $K_{IC}$  by approximately 40% at  $T = 200^\circ\text{C}$  compared to ambient conditions. So, one can argue that, in especially wet rocks, the evaporation of moisture is one of the main conditions for crack closure toughening to occur.

Al-Shayea et al. (2000) studied the fracture toughness under mixed mode loading on a homogenous, muddy limestone. They show an increase of 25% and 9% for  $K_{IC}$  and  $K_{IIIC}$  with increasing temperatures up to 120°C. The applied straight-notched Brazilian Disk experiment was used for the analysis of  $K_{IIIC}$ .

Reopening, coalescence as well as initiation and propagation of grain boundary cracks, due to different thermal expansion of grains and the  $\alpha$ - $\beta$  phase transition of quartz at 573°C, reduces the fracture toughness in further heating phases considerably (c.f. Nasserri et al. (2007) and Duclos & Paquet (1991)). At even higher temperatures intragranular cracks propagate and well-developed crack arrays form. Consequently, the crack dimensions grow throughout the heating process making rock even more vulnerable for fracturing.

The referred workers used different heating rates, different temperature intervals and experimental set-ups than those applied in this work. No mineralogical alterations or ductile behaviour was reported.

### 1.1 The Punch-Through Shear with Confining Pressure experiment

The experimental set-up used in the study is the Punch-Through Shear with Confining Pressure (PTS\CP) experiment. It is suggested that the PTS\CP test utilizes the left over from the ISRM Suggested Method of the Chevron Bend experiment ( $K_{IC}$ ) to obtain  $K_{IIIC}$  from the same sample. Into the cylindrical specimen of diameter equal length (typically 50 mm) notches are drilled centered into the end surfaces. The specimen is placed between a bottom support and a load stamp. During testing the inner cylinder is punched down at a constant displacement rate of 0.2 mm/min inducing a shear load between the drilled-in notches (see Fig. 1 C for specimen geometry and schematic loading). Reaching peak load the notches act as a friction free initiation locus for the propagation of a shear-loaded fracture that connects the notches.

A servo-controlled MTS loading frame establishes the load with a maximum load capacity of 4600 kN, and a stiffness of 11 MN/mm. Confining pressures up to 200 MPa can be applied via a pressure vessel, enabling the PTS\CP experiment to apply confining pressure independently of axial load in comparison to others, i.e. Rao et al. (2003), Ayatollahi & Aliha (2007).

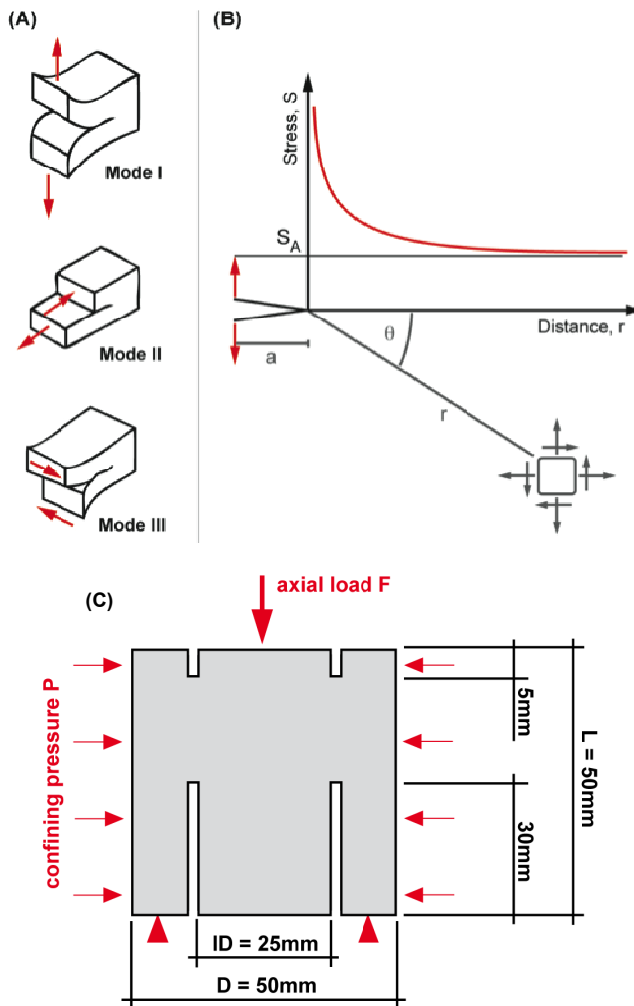


Figure 1. (A) Modes of loading. Mode I: opening mode, Mode II: sliding mode, Mode III: tearing mode. The principle of superposition is sufficient to describe any loading situation. (B) A fracture loaded by a stress  $S_A$  will magnify the stress at the fracture tip. Reaching a critical amount of stress concentration at the fracture tip, the fracture propagates. (C) Specimen geometry and loading scheme of the PTS/CP experiment. The axial load  $F$  punches the inner cylinder down, resulting in a shear-loaded fracture connecting the two notches.

From the maximum applied force  $F_{\max}$  (kN) and the applied confining pressure the Mode II fracture toughness can be calculated using the formula given by

$$K_{IIc} = 0.0378 \cdot \frac{F_{\max}}{A} - 1.795 \cdot 10^{-3} \cdot P \quad (2)$$

where  $A$  ( $\text{mm}^2$ ) is the circular area of the inner cylinder and  $P$  (MPa) is the applied confining pressure. Further background to the methodology can be found in Backers et al. (2002) and Backers (2005).

In this study the specimens are air dried and subsequently placed into an oven at the desired temperature for 12h. Tinfoil prevents a significant temperature loss during transportation from the oven to the loading frame. Measurements on the loss of temperature on the specimen's mantle surface showed a drop of app.  $50^\circ\text{C}$  at  $T = 250^\circ\text{C}$  within 2min. As time of testing is short ( $< 3$  min) temperature loss in the zone of interest, i.e. between the notches, is assumed to be negligible.

### 1.2 Rock material

The grain size of the tested granitic samples from Korea range from 0.1 mm to 3.0 mm with an average grain size of 0.5 mm. The mineralogical composition determined by X-ray diffraction (XRD) analysis classify this rock as a syeno-granite, which is rich in alkali-feldspar (67.2%) with 23% quartz and accessory minerals like biotite (6.9%), muscovite (1.4%), and calcite (1.4%) (Hyung-Mok, 2008). The granite shows green alterations in form of core seize bands. Thin sections show small amounts of pre-existing cracks and weathering (see Fig. 2 B). The Young's modulus is  $29 \pm 1$  GPa, tensile strength is  $10.1 \pm 0.1$  MPa, porosity is about  $1.0 \pm 0.4\%$ , uniaxial compressive strength is  $170 \pm 1$  MPa, and  $K_{IC}$  is  $1.4 \pm 0.1$   $\text{MPa}\sqrt{\text{m}}$  at ambient conditions.

Radial ultrasonic measurements on unheated disc-specimens of the granitic material display an anisotropy of about 15% (see Fig. 2 A and Eq. 3 for calculation).

$$A_v = \frac{v_{p,\max} - v_{p,\min}}{v_{p,\max}} \quad (3)$$

Axial ultrasonic values in all temperature ranges are higher than radial ones, indicating that the majority of microcracks is aligned parallel to the loading direction.

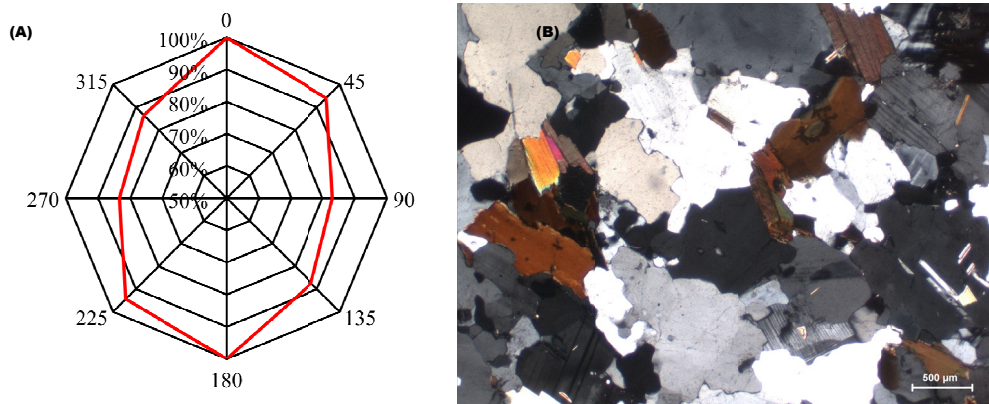


Figure 2. (A) Plot of normalised ultrasonic velocity  $v_p$  in radial direction on disc specimens. The measured  $v_p$  display an anisotropy of about 15%. (B) Thin section of the fine-grained syeno-granite from Korea.

## 2 EXPERIMENTAL RESULTS

A total of 30 specimens was tested at temperatures from 25°C to 250°C in steps of 25°C. No confining pressure was applied to the specimens. Figure 3 A displays the results from the testing. From room temperature up to 150°C,  $K_{IIC}$  is roughly constant at  $3.4 \pm 0.6$  MPa $\sqrt{m}$ ; for  $T > 150^\circ\text{C}$   $K_{IIC}$  increases by approximately 10% to  $3.7 \pm 0.2$  MPa $\sqrt{m}$ . Radial ultrasonic measurements are conducted on specimens prior to and after heating. The difference in p-wave velocity ( $\Delta v_p$ ) increases significantly for  $T > 150^\circ\text{C}$ . Figure 3 B summarizes the results.

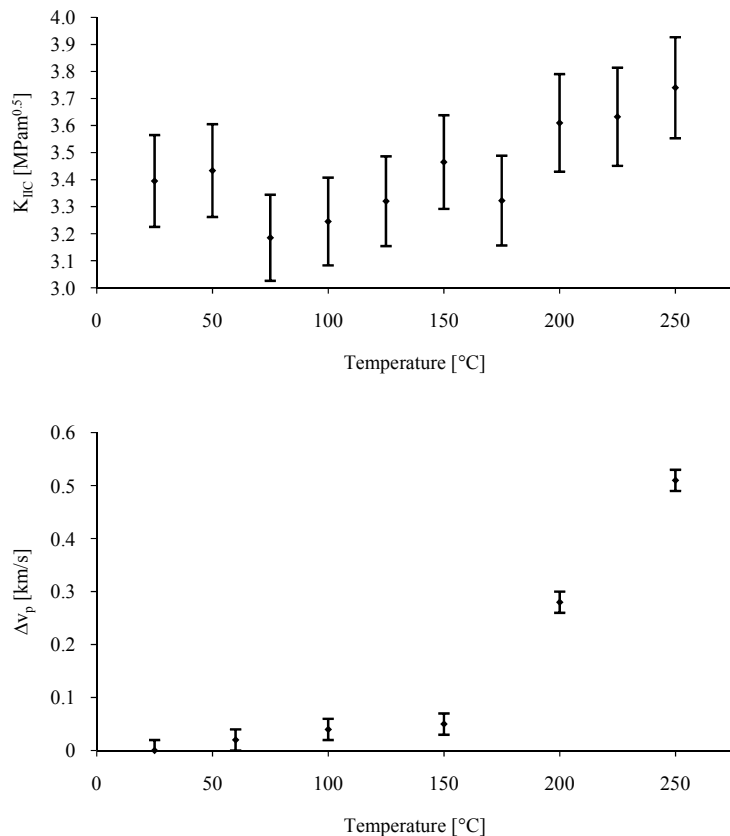


Figure 3. Obtained data from PTS/CP experiment at elevated temperature. Up to 150°C the variation in  $K_{IIC}$  (A) is attributed to anisotropy. At elevated temperatures randomly distributed thermal microcracks increase  $\Delta v_p$  (B) and consequently  $K_{IIC}$ .

## 3 DISCUSSION

Based on Balme et al. (2004), Figure 4 summarises the general relationship between fracture toughness and temperature linked to the microcrack density in the rock. Curve A represents a rock, which is subjected to an increasing temperature for the first time (heat treated). From theory three competing mechanisms are expected during heating when mesoscopic fracture propagating through the rock will interact with the pre-existing and thermally induced microcracks. (A) Generally, the rock resistance towards fracturing decreases when the amount of thermally induced cracks increases. (B) An increase of microcrack density at large angles to the fracture propagation direction can blunt the fracture tip and act as arrester to the propagation. (C) The different thermal expansion of grains may close pre-existing microcracks and strengthen the material.

Curve B in Figure 4 shows the expected response of pre-heat treated material. The processes represented by Curve A have partly been performed in a previous heating cycle. The overall descending trend of fracture toughness is also favored by the decrease of surface energy and enhanced fragile behavior of minerals as they are heated (Darot et al., 1985).

In between these extremes represented by Curve A and B, rocks represented by Curve C might not create new microcracks up to a critical temperature. It is commonly accepted that there exists a threshold temperature below which no thermal fracturing is detectable (c.f. Yong & Wang, 1980). Its value, however, depends on the composition and fabric of the rock. At higher temperatures crack closure toughening or blunting may increase the fracture toughness to a maximum value.

In this study the Mode II fracture toughness and microcrack density, as derived from ultrasonic velocities, remain almost constant for  $T < 150^{\circ}\text{C}$ . Variation of  $K_{IIC}$  can be related to some extent to the natural variation of anisotropy direction.  $K_{IIC}$  can be expected to vary with orientation of microcrack density (Nasseri et al., 2008); lower  $K_{IIC}$  values in this study are assumed to be a product of parallel or subparallel pre-existing microcracks enhancing the Mode II fracture propagation and misaligned microcracks lead to higher values of  $K_{IIC}$ . As was shown by the ultrasonic measurements, the majority of microcracks is orientated in axial direction and the mesoscopic fracture propagates in direction of the orientation of majority of fractures. It is expected that the measured  $K_{IIC}$  is the lower end of possible  $K_{IIC}$  values. The grade of anisotropy however does not depend on temperature (Schön, 2004) and can therefore be neglected in the context of thermal microcracking. This was true for the measured examples, although the absolute crack densities changed considerably. An influence of thermal expansion of grains closing pre-existing fractures is not seen in the measured bulk data at  $25^{\circ}\text{C} < T < 150^{\circ}\text{C}$ . Also the evaporation of possible moisture, which seems to be one of the main conditions for crack closure toughening to occur, is not evident.

The number of microcracks is significantly increased for  $T > 150^{\circ}\text{C}$ . From that a threshold temperature at approximately  $150^{\circ}\text{C}$  is estimated below which no significant thermal microcracking appears (see Figure 4).

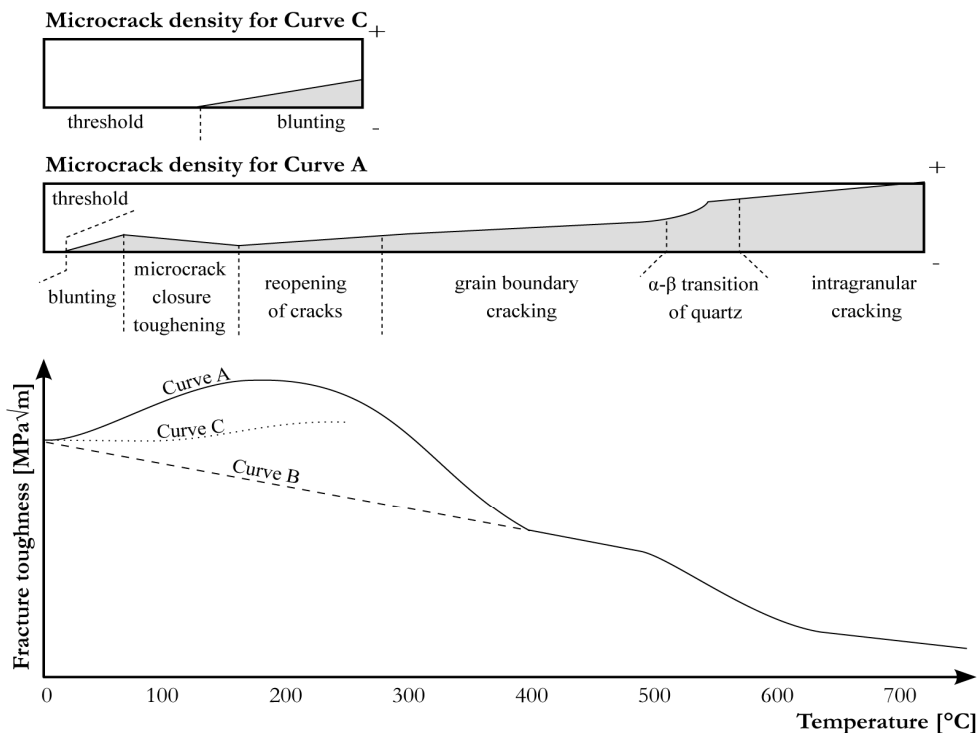


Figure 4. Development of fracture toughness linked to the microcrack evolution during heating for a heat treated rock (Curve A). Curve C represents the results of this study. A likely behavior of a pre-heat treated material is given by Curve B.

As the threshold temperature is on the upper end of reported threshold values it can be argued whether the rock was exposed to temperature cycles previously. Thermal crack damage is assumed to be at its maximum as samples are placed into a pre-heated oven; a discussion of heating rates is beyond the scope of this study but it was reported that thermal microcracking is larger for higher heating rates (Yong & Wang, 1980). The change in ultrasonic velocity in radial direction at above 150°C is attributed to the development of randomly distributed microcracks. Instead of enhancing the passage of the shear-loaded fracture, they act as arrester and a higher energy is needed to overcome this obstacle, hence,  $K_{IIC}$  increases slightly. The increment of  $K_{IIC}$  is small but corresponds to the finding of Al-Shayea et al. (2000) that  $K_{IIC}$  seems to be less dependent on temperature than  $K_{IC}$ .

#### 4 CONCLUSIONS

A total of 30 Punch-Through Shear with Confining Pressure experiments were carried out on fine-grained syeno-granite samples to determine the influence of temperature on Mode II fracture toughness. From the laboratory results and discussion the following conclusions can be drawn:

- It has been shown that the amount of thermally induced microcracks increases significantly for  $T > 150^{\circ}\text{C}$ .
- $K_{IIC}$  for the fine-grained granite increases when heated above 150°C.
- At  $T > 150^{\circ}\text{C}$  the effect of blunting is larger than the effect of fracture-parallel microcracks.
- The difference in ultrasonic velocities prior and after heating proved to be a good indicator to the development of thermal microcracks.

#### ACKNOWLEDGMENT

The work was carried out partly in the context of an international research and development project aiming at further development of a coupled thermo-hydro-mechanical fracture mechanics software called fracod2D. The project is sponsored and carried out by CSIRO, Australia, SK Engineering and Geology, Korea, KIGAM, Korea, Fracom Oy., Finland, Leibniz-Institut for Applied Geophysics (LIAG), Germany, and GeoFrames GmbH, Germany. Further support to the work was granted by the European Union, European Fund for Regional Development, program 'Investment to Future', Period 2007-2013. The rock material for this study was kindly provided by KIGAM.

#### REFERENCES

- Al-Shayea, N.A., Khan, K. & Abduljauwad S.N. 2000. Effects of confining pressure and temperature on mixed-mode (i-ii) fracture toughness of a limestone rock. *International Journal of Rock Mechanics and Mining Science* 37: 629-643.
- Atkinson, B.K. (ed.) 1987. *Fracture mechanics of rocks*. Academic press geology series. London: Academic Press.
- Ayatollahi, M.R. & Aliha, M.R.M. 2007. Fracture toughness study for a brittle rock subjected to mixed mode I/II loading. *International Journal of Rock Mechanics and Mining Science* 44: 617-624.
- Backers, T., Stephansson, O. & Rybacki, E. 2002. Rock fracture toughness testing in mode II punch-through shear test. *International Journal of Rock Mechanics and Mining Science* 39: 755-769.
- Backers, T. 2005. Fracture Toughness Determination and Micromechanics of rock under mode I and mode II loading. *PhD thesis*, University of Potsdam, Germany.
- Balme, M.R., Rocchi, V., Jones, C., Sammonds, P.R., Meredith, P.G. & Boon, S. 2004. Fracture toughness measurements on igneous rocks using a high- pressure, high- temperature rock fracture mechanics cell. *Journal of Volcanic Geothermal Research* 132: 159-172.

- Byfut, A., Schroeder, A., Carstensen, C. & Backers, T. 2009. Simulation of Crack Propagation by the Extended Finite Element Method with Application in Geomechanics. *EAGE 71th Conference and Exhibition, Amsterdam, The Netherlands*.
- Darot, M., Gueguen, Y. & Benchemam, Z. 1985. Ductile - brittle transition investigated by micro-indentation: results for quartz and olivine. *Physics of the Earth and Planetary Interiors* 40: 180 – 186.
- Duclos, R. & Paquet, J. 1991. High temperature behavior of basalt role of temperature and strain rate on compressive strength and kic toughness of partially glassy basalt at atmospheric pressure. *International Journal of Rock Mechanics and Mining Science* 28: 71-76.
- Dwivedi, R.D., Goel, R.K., Prasad, V.V.R. & Sinha, A. 2000. Thermo-mechanical properties of indian or other granites. *International Journal of Rock Mechanics and Mining Science* 45: 303-315.
- Fredrich, J.T. & Wong, T. 1986. Micromechanics of thermally induced cracking in three crustal rocks. *Journal of Geophysical Research* 91(B12): 743-764.
- Funatsu, T., Seto, M., Shimada, H., Matsui, K. & Kuruppu, M. 2004. Combined effects of increasing temperature and confining pressure on the fracture toughness of clay bearing rocks. *International Journal of Rock Mechanics and Mining Science* 41: 927-938.
- Hyung-Mok, K. 2008. Summary of previous laboratory test results of kigam's. *Technical report*, Korea Institute of Geoscience & Mineral Resources.
- Meredith, P.G. & Atkinson, B.K. 1985. Fracture toughness and subcritical crack growth during high-temperature tensile deformation of westerly granite and black gabbro. *Physics of the Earth and Planetary Interiors* 39: 33-51.
- Nasseri, M.H.B., Schubnel, A. & Young, R.P. 2007. Coupled evolutions of fracture toughness and elastic wave velocities at high crack density in thermally treated westerly granite. *International Journal of Rock Mechanics and Mining Science* 44: 601-616.
- Nasseri, M.H.B. & Mohanty, B. 2008. Fracture toughness anisotropy in granitic rocks. *International Journal of Rock Mechanics & Mining Sciences* 45: 167-193.
- Rao, Q., Sun, Z., Stephansson, O., Li, C. & Stillborg, B. 2003. Shear fracture (Mode II) of brittle rock. *International Journal of Rock Mechanics and Mining Science* 40: 355-375.
- Lawn, B. 1993. *Fracture of brittle solids – second edition*. Cambridge: Cambridge University Press.
- Ravalec, M., Darot, M., Reuschle, T. & Gueguen, Y. 1996. Transport properties and microstructural characteristics of a thermally cracked mylonite. *Pageoph* 146(2): 207-227.
- Reuschle, T., Haore, S.G. & Darot, M. 2006. The effect of heating on the microstructural evolution of la peyrate granite deduced from acoustic velocity measurements. *Earth and Planetary Science Letters* 243: 692-700.
- Schoen, J.H. 2004. *Physical properties of rocks - Fundamentals and principles of petrophysics*. Volume 18, Handbook of geophysical exploration of Seismic exploration. Oxford: Elsevier.
- Stephansson, O., Shen, B., Rinne, M., Amemiya, K., Yamashi, R. & Toguri, S. 2008. FRACOD Modeling of Rock Fracturing and Permeability Change in Excavation Damaged Zones. *International Association for Computer Methods and Advances in Geomechanics; proc. of the 12th International Conference, Goa, 1-6 October*.
- Whittaker, B.N., Singh, R.N. & Sun, G. 1992. *Rock Fracture Mechanics, Principles, Design and Applications*. Amsterdam: Elsevier.
- Yong, C. & Wang, C. 1980. Thermally induced acoustic emission in westerly granite. *Geophysical Research Letters* 7(12): 1089-1092.
- Zhang, Z.X., Yu, J., Kou, S.Q. & Lindqvist, P.A. 2001. Effects of high temperatures in dynamic rock fracture. *International Journal of Rock Mechanics and Mining Science* 38: 211-225.